

Supporting Information

Chris Neale^{a,b}, Hamed Ghanei^c, John Holyoake^{a,d}, Russell E. Bishop^e, Gilbert G. Privé^{b,c,d}, Régis Pomès^{a,b,1}

^aMolecular Structure and Function, The Hospital for Sick Children, 555 University Avenue, Toronto, Ontario, M5G 1X8, Canada

Departments of ^bBiochemistry and ^cMedical Biophysics, University of Toronto, 101 College Street, Toronto, Ontario, M5G 1L7, Canada

^dOntario Cancer Institute and Campbell Family Cancer Research Institute, UHN, 101 College Street, Toronto, Ontario, M5G 1L7, Canada

^eDepartment of Biochemistry and Biomedical Sciences and Michael G. DeGroot Institute for Infectious Disease Research, McMaster University, Hamilton, Ontario, L8N 3Z5, Canada

¹Corresponding author: Régis Pomès, Hospital for Sick Children, 555 University Avenue, Toronto, Ontario, M5G 1X8, Canada; E-mail: pomes@sickkids.ca; Tel.: 1-416-813-5686; Fax: 1-416-813-5022

SI Figure

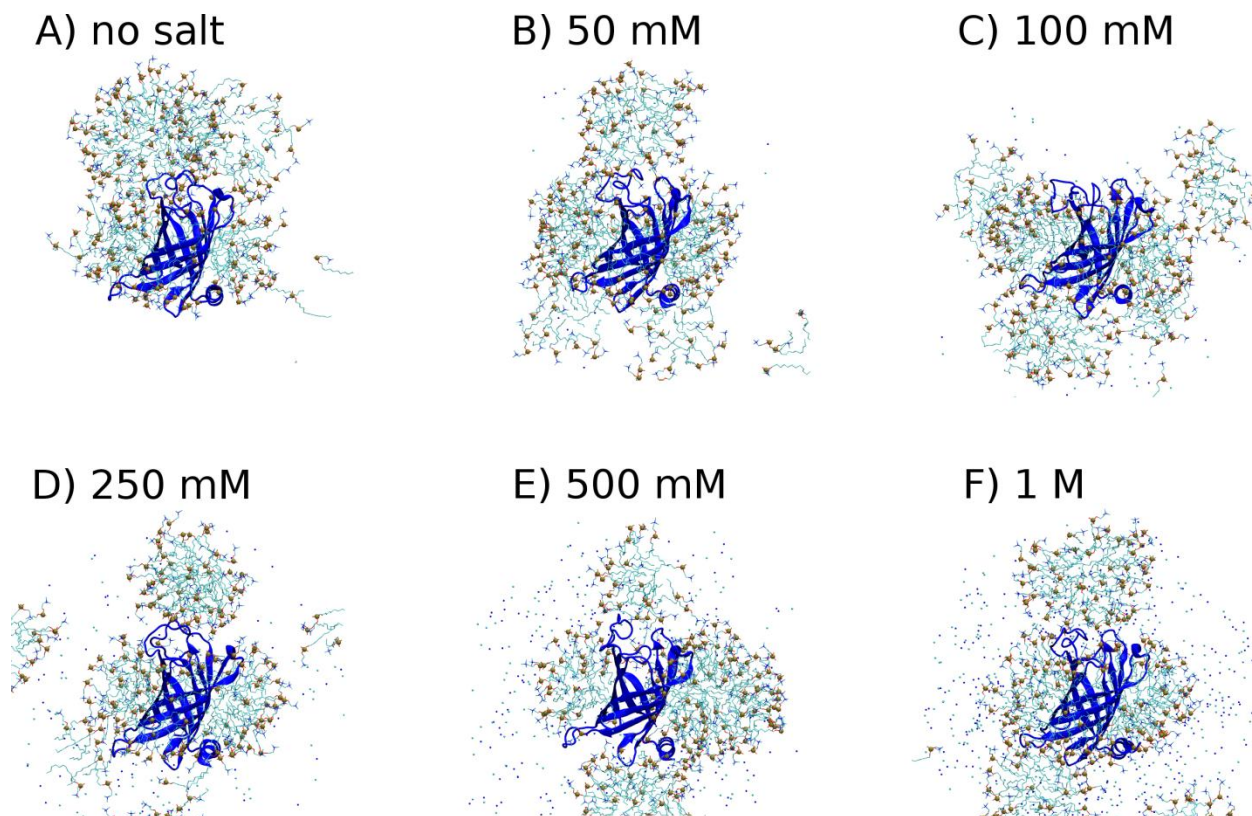


Figure S1: Apical interactions of PagP with detergent micelles form and persist in simulations with salt concentrations up to 1 M. Snapshots obtained after 250 ns of simulation. PagP is shown as a blue cartoon and DPC detergent molecules are shown as sticks that are coloured for (cyan) carbon, (blue) nitrogen, (red) oxygen, and (brown with sphere) phosphorus atoms. Salt ions are shown as small (Na^+) blue and (Cl^-) cyan spheres. Large salt crystals formed in ≤ 50 ns in simulations with salt concentrations ≥ 2 M (data not shown).

SI Movie Captions

Movie S1: One of the six 500-ns trajectories of PagP and DPC detergents obtained in this work. In this trajectory, all four molecule of PagP condense into a single large aggregate. The four molecules of PagP in the central unit cell, as well as their periodic images, are shown as red cartoons. Detergent molecules are shown as grey lines. Water molecules and ions are omitted for clarity. Atomic positions have been time-averaged to facilitate the identification of global motions.

Movie S2: One of the six 500-ns trajectories of PagP and DPC detergents obtained in this work. After 500 ns, there are two large aggregates, each containing two molecules of PagP. Molecules of PagP and DPC are coloured red or blue, and pink or cyan, respectively, based on their molecular aggregate at the 500-ns timepoint. Periodic images are shown and coloured similarly. Water molecules and ions are omitted for clarity. Atomic positions have been time-averaged to facilitate the identification of global motions.

Movie S3: Spatial distribution of detergent and protein molecules around a central molecule of PagP. The spatial distribution function (SDF) depicts the time- and ensemble-averaged arrangement of (cyan) detergent and (red) protein molecules around a (black cartoon) central molecule of PagP. The isodensity surface of other protein molecules is drawn at a lower density value than is the isodensity surface of detergent molecules. This makes the red protein surface more prominent in that it encloses a larger area than it would if all contours were drawn at the same density value. This was done in order to show more of the protein arrangements that were produced by detergent-mediated protein aggregation so as to include those arrangements that occurred infrequently.

SI Methods

Parameterization of LDAO. The crystal structure of PagP in LDAO (PDB ID 1THQ) has a single molecule of LDAO bound within the hydrocarbon ruler¹. To model this detergent, we constructed a united atom representation of LDAO by mimicking the Berger lipid parameters² for POPC³. Specifically, parameters for bonds, angles, and dihedrals were taken from the Berger parameters for a lipid-headgroup choline group and a saturated acyl chain². The atomic nomenclature used to determine the bonded and non-bonded interactions is depicted in Fig. S2. Lennard-Jones values for the oxygen atom were set to those of the fatty acid carbonyl oxygen in POPC. The equilibrium length of the N-O bond was taken from the molecule of LDAO in the hydrocarbon ruler in the 1THQ structure (0.125 nm). Other bonded parameters involving the O-N bond (bond-length force constant and parameters for O-N-C angles and O-N-C-C dihedrals) were set to those involving (CH₃)-N in the Berger choline group. Bonded parameters for the junction between the dimethyl amine oxide headgroup of LDAO and its lauryl chain were obtained from the Berger lipid parameters² for POPC³, substituting different Berger atom types where necessary. A complete list of the applied bonded parameters that are required by LDAO, but are not provided by POPC, is provided in Table S1.

To obtain partial charges, two molecules of LDAO were constructed with PyMOL⁴, both in all-*trans* acyl-chain conformations. These two conformations differed in the O-N-C-C dihedral angle, which was either 180° or 60°. Mulliken charges⁵ were computed for each of these conformations with RHF/6-31G* quantum mechanical basis set using the Gaussian 98 program⁶ after steepest-descent geometry optimization using the same basis set while fixing the O-N-C-C dihedral angle. Partial charges obtained from these two computations are shown in Figs. S3A, B. Because partial charges are conformationally invariant during our simulations, the partial charges obtained from each starting conformation of LDAO were averaged and rounded to a single significant digit. This yielded the partial charges that we used in simulations involving LDAO, which are shown in Fig. S3C.

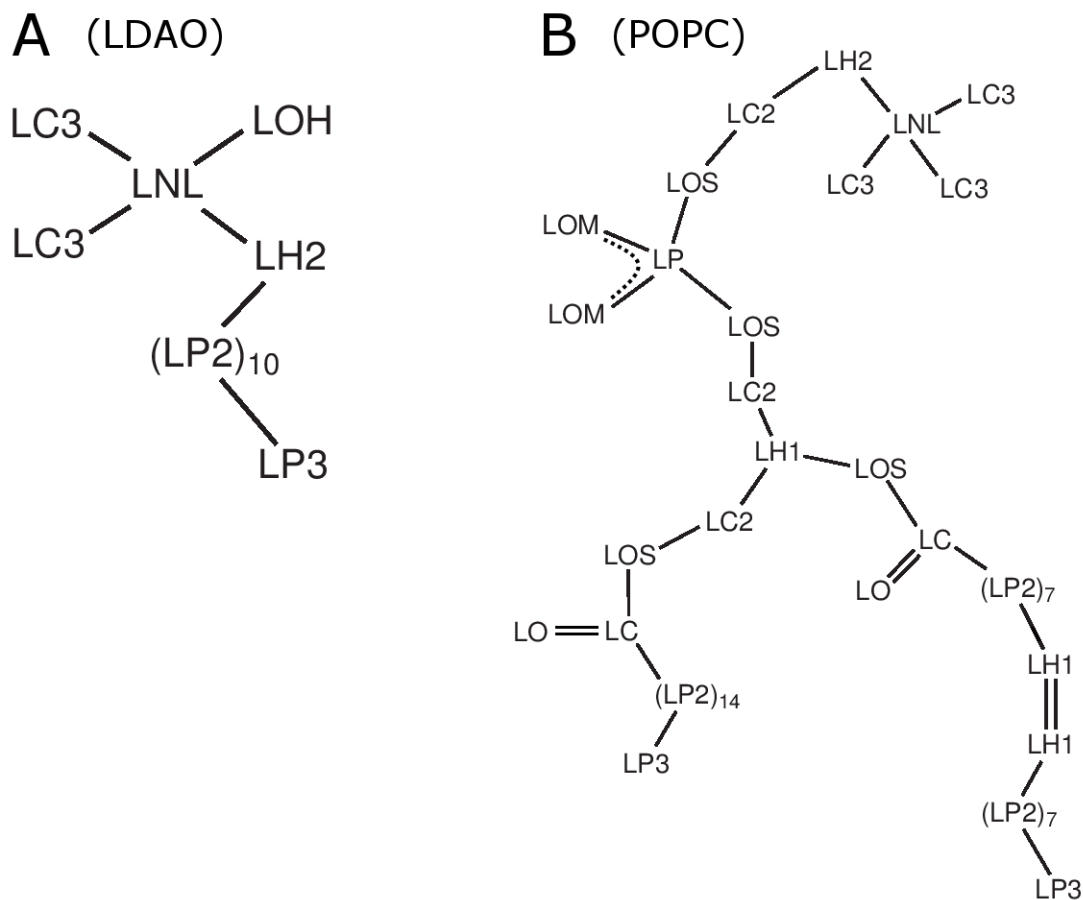


Figure S2: Atom types used to determine the bonded interactions of (A) LDAO and (B) POPC. The simulation system did not contain POPC, which was used as a template to derive LDAO parameters. Atom type designations follow the nomenclature of the lipid.itp file obtained from the website of Peter Tieleman⁷. Numerical values can be found in the lipid.itp file and the work of Berger *et al.*², using the atom naming outlined in this Figure, given the modifications outlined in Table S1. Molecular representations were created with ChemDraw.

Table S1: Bonded parameters required by LDAO that are not provided by POPC, and the parameters that were used in their place. This united-atom representation of LDAO was constructed to mimic the Berger lipid parameters² for POPC³. Atom type designations follow the nomenclature of the lipid.itp file obtained from the website of Peter Tieleman⁷. Numerical values can be found in the lipid.itp file and the work of Berger *et al.*², using the atom naming outlined in Fig. S2, given the modifications outlined in this table.

Unavailable parameters	Used parameters
<i>Lennard-Jones</i>	
LOH	LO
<i>Bonds</i>	
LNL-LOH	$b_0=0.125$ nm; $k_b=LNL-LC3$ ^a
LH2-LP2	LP2-LP2
<i>Angles</i>	
LOH-LNL-LC3	LC3-LNL-LC3
LOH-LNL-LH2	Taken from CHARMM27 LDAO parameters ^b
LNH-LH2-LP2	LNH-LH2-LC2
LH2-LP2-LP2	LP2-LP2-LP2
<i>Dihedrals</i>	
LOH-LNL-LH2-LP2	Omitted ^c
LC3-LNL-LH2-LP2	LC3-LNL-LH2-LC2
LNL-LH2-LP2-LP2	LC-LP2-LP2-LP2
LH2-LP2-LP2-LP2	LC-LP2-LP2-LP2

(a) b_0 is the equilibrium bond length, k_b is the bond stretching force constant. The equilibrium bond length was obtained from PDB ID 1THQ. The bond stretching force constant was not applied during these simulations because all bond lengths were holonomically constrained.

(b) $\theta_0=113^\circ$; $k_\theta=670$ kJ/mol/rad² (θ_0 is the equilibrium angle, and k_θ is the angle stretching force constant).

(c) The dihedral angle of LOH-LNL-LH2-LP2 was not included in the Hamiltonian.

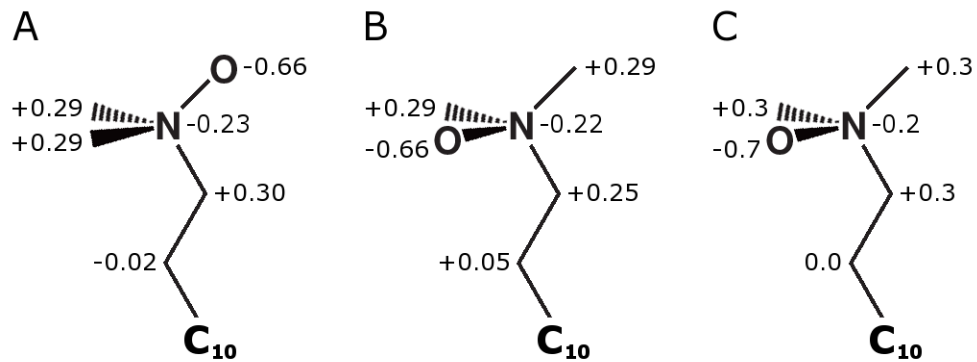


Figure S3: Charge determination for LDAO in an all-*trans* acyl-chain conformation. Charges were determined with the O-N-C-C dihedral angle set to (A) 180° or (B) 60°. (C) Selected charges for use in MD simulations. In all cases, the distal 10 carbons of the acyl chain were uncharged.

SI References

1. Ahn, V. E.; Lo, E. I.; Engel, C. K.; Chen, L.; Hwang, P. M.; Kay, L. E.; Bishop, R. E.; Privé, G. G., A hydrocarbon ruler measures palmitate in the enzymatic acylation of endotoxin. *EMBO J.* **2004**, *23* (15), 2931-2941.
2. Berger, O.; Edholm, O.; Jähnig, F., Molecular dynamics simulations of a fluid bilayer of dipalmitoylphosphatidylcholine at full hydration, constant pressure, and constant temperature. *Biophys. J.* **1997**, *72* (5), 2002-2013.
3. Tieleman, D. P.; Forrest, L. R.; Sansom, M. S. P.; Berendsen, H. J. C., Lipid properties and the orientation of aromatic residues in OmpF, influenza M2, and alamethicin systems: molecular dynamics simulations. *Biochemistry* **1998**, *37* (50), 17554-17561.
4. DeLano, W. L. *The PyMOL molecular graphics system*, DeLano Scientific, San Carlos, CA.: 2002.
5. Mulliken, R. S., Electronic population analysis on LCAO[single bond]MO molecular wave functions. II. Overlap populations, bond orders, and covalent bond energies. *J. Chem. Phys.* **1955**, *23* (10), 1841-1846.
6. Frisch, M. J.; Trucks, G. W.; Schlegel, H. B.; Scuseria, G. E.; Robb, M. A.; Cheeseman, J. R.; Zakrzewski, V. G.; Montgomery, J. A., Jr., ; Stratmann, R. E.; Burant, J. C.; Dapprich, S.; Millam, J. M.; Daniels, A. D.; Kudin, K. N.; Strain, M. C.; Farkas, O.; Tomasi, J.; Barone, V.; Cossi, M.; Cammi, R.; Mennucci, B.; Pomelli, C.; Adamo, C.; Clifford, S.; Ochterski, J.; Petersson, G. A.; Ayala, P. Y.; Cui, Q.; Morokuma, K.; Malick, D. K.; Rabuck, A. D.; Raghavachari, K.; Foresman, J. B.; Cioslowski, J.; Ortiz, J. V.; Stefanov, B. B.; Liu, G.; Liashenko, A.; Piskorz, P.; Komaromi, I.; Gomperts, R.; Martin, R. L.; Fox, D. J.; Keith, T.; Al-Laham, M. A.; Peng, C. Y.; Nanayakkara, A.; Gonzalez, C.; Challacombe, M.; Gill, P. M. W.; Johnson, B.; Chen, W.; Wong, M. W.; Andres, J. L.; Gonzalez, C.; Head-Gordon, M.; Replogle, E. S.; Pople, J. A. *Gaussian 98, Revision A.6*, Pittsburgh, 1998.
7. Tieleman, D. P., http://moose.bio.ucalgary.ca/index.php?page=Structures_and_Topologies, accessed July 16, 2009.